

PAPER • OPEN ACCESS

Stimulated emission and absorption of photons in magnetic point contacts

To cite this article: Yu G Naidyuk *et al* 2012 *New J. Phys.* **14** 093021

View the [article online](#) for updates and enhancements.

Related content

- [Hot electrons in magnetic point contacts as a photon source](#)
A M Kadigrobov, R I Shekhter, S I Kulnich *et al.*
- [Microwave-induced direct spin-flip transitions in mesoscopic Pd/Co heterojunctions](#)
Torsten Pietsch, Stefan Egle, Martin Keller *et al.*
- [Spin laser based on magnetic nano-contact array](#)
V. Korenivski, A. Iovan, A. Kadigrobov *et al.*

Recent citations

- [Wurtzite spin lasers](#)
Paulo E. Faria Junior *et al*
- [Microwave-induced direct spin-flip transitions in mesoscopic Pd/Co heterojunctions](#)
Torsten Pietsch *et al*
- [Spin laser based on magnetic nano-contact array](#)
V. Korenivski *et al*

Stimulated emission and absorption of photons in magnetic point contacts

Yu G Naidyuk^{1,8}, O P Balkashin¹, V V Fisun¹, I K Yanson¹,
A Kadigrobov^{2,3}, R I Shekhter², M Jonson^{2,4,5}, V Neu⁶,
M Seifert⁶, S Andersson⁷ and V Korenivski⁷

¹ B I Verkin Institute for Low Temperature Physics and Engineering,
National Academy of Sciences of Ukraine, 47 Lenin Avenue,
61103 Kharkiv, Ukraine

² Department of Physics, University of Gothenburg, SE-412 96 Göteborg,
Sweden

³ Theoretische Physik III, Ruhr-Universität Bochum, D-44801 Bochum,
Germany

⁴ SUPA, Institute of Photonics and Quantum Sciences, Heriot-Watt University,
Edinburgh EH14 4AS, UK

⁵ Department of Physics, Division of Quantum Phases and Devices,
Konkuk University, Seoul 143-701, Korea

⁶ Leibniz-Institut für Festkörper- und Werkstofforschung Dresden e.V.,
Postfach 270116, D-01171 Dresden, Germany

⁷ Nanostructure Physics, Royal Institute of Technology, 10691 Stockholm,
Sweden

E-mail: naidyuk@ilt.kharkov.ua

New Journal of Physics **14** (2012) 093021 (10pp)

Received 19 June 2012

Published 13 September 2012

Online at <http://www.njp.org/>

doi:10.1088/1367-2630/14/9/093021

Abstract. Point contacts between high anisotropy ferromagnetic SmCo₅ and normal metal Cu are used to achieve a strong spin-population inversion in the contact core. Subjected to microwave irradiation in resonance with the Zeeman splitting in Cu, the inverted spin population relaxes through stimulated spin-flip photon emission, detected as peaks in the point-contact resistance. Resonant

⁸ Author to whom any correspondence should be addressed.



Content from this work may be used under the terms of the [Creative Commons Attribution-NonCommercial-ShareAlike 3.0 licence](https://creativecommons.org/licenses/by-nc-sa/3.0/). Any further distribution of this work must maintain attribution to the author(s) and the title of the work, journal citation and DOI.

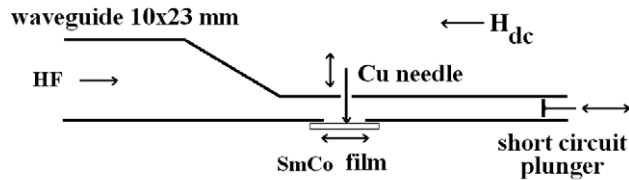
spin-flip photon absorption is detected as resistance minima, corresponding to sourcing the photon field energy into the electrical circuit. These results demonstrate fundamental mechanisms that are potentially useful in designing metallic spin-based lasers.

S Online supplementary data available from stacks.iop.org/NJP/14/093021/mmedia

At the core of spin electronics are magnetic nanostructures utilizing spin-polarized electron currents for achieving novel functionality for devices such as field sensors [1, 2] and magnetic random access memory elements [3, 4]. Of particular interest is the case when a highly non-equilibrium spin population can be created and used to produce radiation (emission of photons). Spin injection into semiconductors has been reported to result in the emission of circularly polarized light [5, 6] and is used to measure the spin polarization of the injected current. In the case when the electron transition emitting a photon is between two levels that are spin-split by an external field [6], however, the semiconductor's energy gap plays no role—the spin splitting produces two subbands within the conduction band. Based on this observation, some of us have proposed a new concept for a solid-state THz laser based on a population inversion of spin-split levels in a ferromagnetic metal [7]. The spin population is inverted by injecting spin-polarized currents through a tunnel barrier or a nano-constriction in such a way that electrons are either pumped into the upper spin-split level or pumped out of the lower one. When the injection region is resonantly irradiated, stimulated photon emission takes place and is predicted to reach giant optical gain levels due to the vastly higher electron density in metals compared to semiconductors. If the photon emission rate can be made to exceed the photon absorption rate, the metal becomes transparent to the radiation and acts as a laser. The role of the energy gap in semiconductor-based lasers is played by the exchange- or Zeeman spin-split energy levels in the metallic active region for ferromagnetic (F)- and normal metal (N)-based lasers, respectively. The realization of such spin-based metallic THz and microwave lasers and masers would be a breakthrough in the field. A recent experiment using this new laser concept [7] has been interpreted in terms of photon emission by spin-flip relaxation of exchange-split spin levels in a ferromagnetic metal [8]. The resonant character of the detected THz radiation remains to be demonstrated however.

In this paper, we focus on the case when the active region is a normal metal with electron spin levels Zeeman-split by an external magnetic field and the corresponding radiation frequency in the microwave range. Magnetic point contacts (PCs) provide the ideal system for demonstrating the proposed effects, making possible very high injection current densities ($\sim 10^9$ A cm⁻²) into very small active volumes (1–10 nm diameter). Furthermore, PC spectroscopy [9] allows *in-situ* monitoring of the relaxation processes taking place in the contact core. Using a high anisotropy spin injector, SmCo₅, we significantly extend our earlier result [10] on *stimulated emission of microwave radiation* by a metallic PC and demonstrate the mirror effect of spin-flip *photon absorption*. In addition, we extend the modeling of these spin-photo-electronic effects by incorporating into the theory of [10] realistic non-photon spin relaxation in the active region.

WAVEGUIDE HOLDER



STANDING WAVE PICTURE

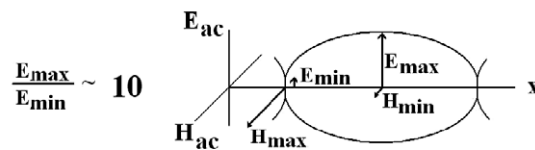


Figure 1. Schematic diagram of the waveguide PC holder, showing the position of the sample (film) and the tip (Cu). A short-circuit plunger is used to tune the standing wave maxima to the PC position.

SmCo₅ epitaxial films were prepared by pulsed laser deposition on Cr-buffered MgO(110) substrates with the *c*-axis (magnetic easy axis) aligned along one in-plane substrate edge. Film preparation and crystallographic and magnetic properties are comparable to samples described in [11], and the Cr capping layer was replaced by a Cu capping layer of about 3–5 nm in thickness. The SmCo₅ films were 50 nm thick, with the rms roughness of approximately 3 nm. They possess extremely large uniaxial magnetocrystalline anisotropy ($K_u \approx 10 \text{ MJ m}^{-3}$) and a saturation polarization of about 1 T, comparable to the respective values in single crystals, and display a sharp magnetization switching along the easy axis at coercive fields of 3–6 T. Thus, applying a reversing field of up to 1 T leaves the magnetization unchanged while producing a strong *inverse* Zeeman splitting in a normal-metal PC to the surface of the film. Such tip–surface type PCs were produced directly in liquid helium using a precision positioning mechanism, making it possible to *in-situ* change the location of the surface contact and the clamping force acting on the tip. The resistance of the contacts was in the range of 10–30 Ω , corresponding to a PC diameter of 10–5 nm [9]. In searching for the effect of photon emission/absorption in the magneto-transport properties of PCs, under external magnetic fields and radiofrequency (RF) irradiation, we have used two experimental methods of detection. The first one is the measurement of differential resistance dV/dI using a synchronous detection of an ac voltage proportional to the first harmonic of the small (about 0.1 mV) modulating bias voltage with a frequency of about 1 kHz applied to a PC. The second method is by detection of a rectification signal V_{det} synched to the chopping frequency of the RF power irradiating the PC (400 Hz; for details of the measurement schematics, see the supplementary material, available from stacks.iop.org/NJP/14/093021/mmedia). Magnetic fields of –5 to 5 T in the film plane were produced using a superconducting solenoid. Negative polarity of the bias voltage corresponds to electron injection from the tip into the film. A microwave field was applied to the PCs using a $10 \times 23 \text{ mm}^2$ X-band waveguide with a smooth transition to a $2 \times 23 \text{ mm}$ cross section, as illustrated in figure 1. The change in the PC resistance caused by microwave irradiation, V_{det} ,

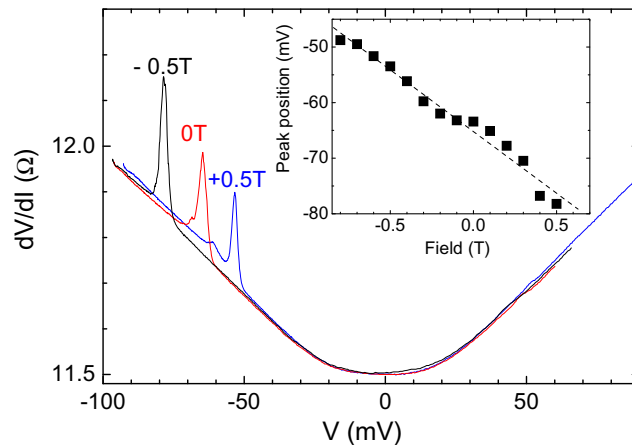


Figure 2. Differential resistance of a SmCo_5/Cu PC with $R = 11.5 \Omega$ versus bias voltage at three magnetic fields. The inset shows the position of the STT peak versus magnetic field, with the dashed line representing a linear fit.

was measured using a lock-in technique where the microwave power was modulated at low frequency taken as the reference for V_{det} [12].

We first calibrate the obtained SmCo_5/Cu PCs with respect to the now well understood effect of spin-transfer-torque (STT)-driven magnetization dynamics caused by the secondary spin polarization in the PC core [12–14]. At high bias voltages applied to a PC, typically in excess of 50 mV for 5–10 nm contacts (the 20 Ω contact resistance range), the spin accumulation at the F/N interface can become sufficiently high to cause a spin-wave instability (magnon excitation) and lead to a magnetization precession in the PC core, which is manifested through peaks in the differential resistance for the electron flow from the normal metal into the ferromagnet (negative bias voltage), such as shown in figure 2. The position of these peaks is dictated by the effective anisotropy acting on the ferromagnetic contact core, which in the case of SmCo_5 is the high intrinsic anisotropy of the material. A moderate applied magnetic field acts to enforce or compensate for this effective anisotropy, which results in shifting the position of the STT peak along the bias voltage direction—more bias and therefore a stronger spin torque is required to excite the core magnetization subject to a higher anisotropy, and less spin torque is needed when the anisotropy is reduced by the opposing field. Thus, the applied field of 0.5 T shifts the STT maximum by approximately a tenth along the voltage axis, which is to be expected for the intrinsic anisotropy of the material of several tesla. The STT peak position as a function of the applied field is shown in the inset of figure 2. The linear dependence observed agrees well with the expected behavior for STT dynamics and, importantly, the peak continues to be observed and its position changes monotonically as the field changes sign. These results show that the current through the SmCo_5/Cu PCs under study is spin polarized and produces a significant spin accumulation in the contact core. Below we use this strong spin accumulation to demonstrate a new regime in magnetic PCs and a new effect based on photon-emitting and photon-absorbing spin-flip transitions, rather than magnon excitation responsible for the STT effect.

Figure 3 illustrates four basic spin-flip photon emission/absorption processes in a magnetic PC. For a majority ferromagnetic injector, such as SmCo_5 , the electrons injected into the normal metal (N) have their magnetic moment along the magnetization \mathbf{M} of the ferromagnet (F). With

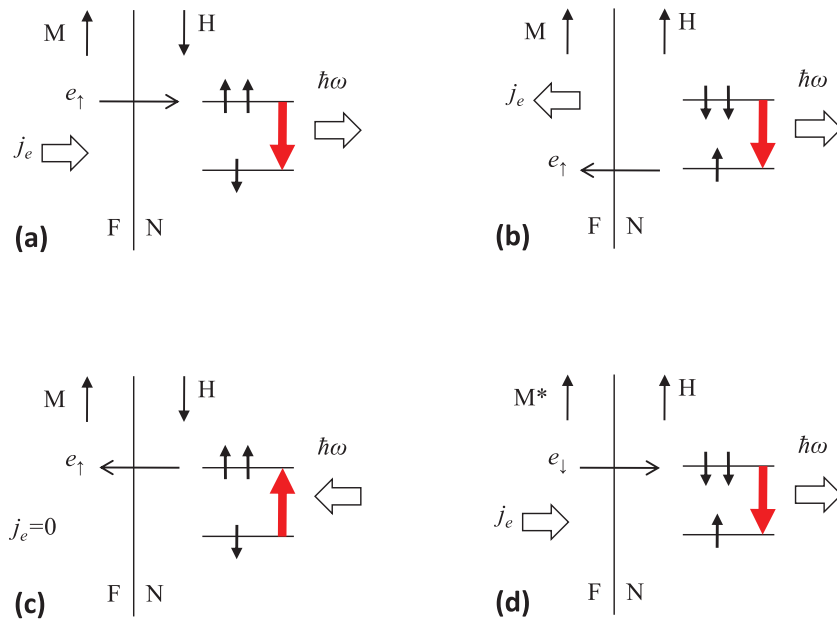


Figure 3. Schematic diagram of four spin-flip transitions accompanied by photon emission or absorption: (a) the magnetization \mathbf{M} and applied field \mathbf{H} are antiparallel, majority electrons in the ferromagnet F are injected into the normal metal N, leading to an inverse population of the Zeeman levels in N. A spontaneous or stimulated spin-flip transition emits a photon with frequency corresponding to the spin splitting; (b) \mathbf{M} and \mathbf{H} are parallel, electrons are injected from N predominantly into the majority band of F, resulting in inversely populated Zeeman levels in N; (c) \mathbf{M} and \mathbf{H} are antiparallel, no voltage bias is applied to the contact, absorption of photons at the frequency of the spin splitting in N produces an overpopulation of electrons having moments along the high-conductivity majority spin channel of F and thereby a flow of electrons through the interface (a photocurrent); (d) F is of the minority type as indicated by the asterisk, \mathbf{M} and \mathbf{H} are parallel, a spin-minority current inversely populates the Zeeman levels in N, which undergo spin-flip relaxation through photon emission. Small arrows denote the direction of the electron's magnetic moment.

the external field applied antiparallel to \mathbf{M} , as in figure 3(a), the electrons injected into the normal metal populate the high-energy Zeeman level there, which leads to an inverse population of the two spin-split levels. This inverse population is not in equilibrium but maintained by the bias current through the PC. Intrinsic spin relaxation in such weak spin-orbit non-magnetic metals as Cu is relatively slow, so spin-flip relaxation through emission or absorption of photons can be dominant. Figure 3(b) shows the same photon emission process, but now for an electron flow from the normal metal to the ferromagnet and an external field applied parallel to the magnetization. The majority-spin subband in the ferromagnet contains more electron states than the minority-spin subband and hence majority-spin electrons carry most of the current through the N/F interface. This preferentially depopulates the lower-energy Zeeman level in the normal metal and thereby creates a spin-population inversion, which can decay through photon emission. Photon absorption by a spin-flip process is illustrated in figure 3(c), where the external

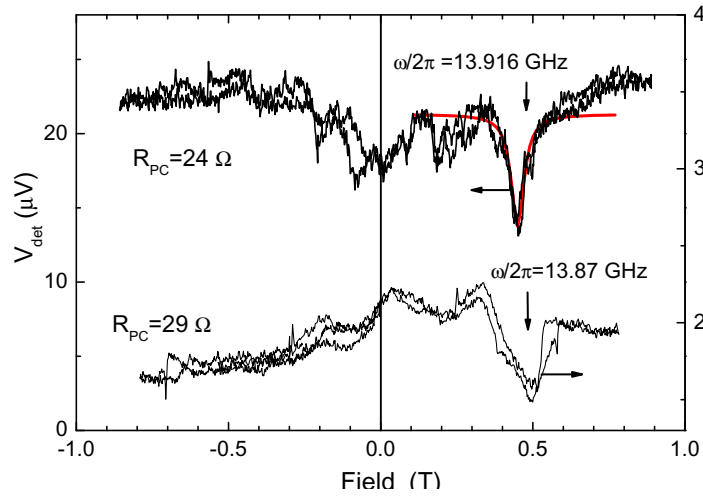


Figure 4. Detected voltage V_{det} (see text) versus magnetic field for two unbiased SmCo_5/Cu PCs subject to 13.9 GHz microwave irradiation at $T = 4.2$ K. Vertical arrows indicate resonant field values H_{res} for which the photon energy $\hbar\omega = 2g\mu_s H_{\text{res}}$ if $g = 2$ and $s = 1/2$. Minima in V_{det} correspond to minima in the PC resistance. The red (smooth) curve is a theoretical fit according to equation (1).

field is antiparallel to \mathbf{M} and no bias is applied to the contact. The equilibrium, equally populated spin levels in the normal metal are subject to a microwave field with frequency in resonance with the Zeeman splitting. Absorption of a microwave photon by an electron induces a spin-flip transition from the low-energy to the high-energy Zeeman level, which overpopulates the high-conductivity majority spin channel of the N/F interface and thereby produces a photo-current. A variation of the photon emission schemes of figures 3(a) and (b) is illustrated in figure 3(d), where the field and magnetization are parallel and the injector is a minority ferromagnet, such as Fe–Cr alloy [15].

The injected electrons, now having magnetic moments opposite to \mathbf{M} , populate the high-energy Zeeman level in the normal metal and the resulting spin-population inversion can lead to photon emission [10]. It is clear that the majority injector schemes require a high anisotropy material, whereas the minority injector configuration can be implemented with a soft ferromagnet as well. Below we demonstrate these fundamental spin-photo-electronic effects using 5–10 nm scale PCs and a high anisotropy spin-majority injector.

We start by demonstrating the photon absorption effect illustrated in figure 3(c). This configuration requires that a magnetic field, of sufficient strength to achieve a Zeeman splitting of reasonable magnitude, is antiparallel to the magnetization of the injector. Therefore, a very high anisotropy material, such SmCo_5 with a coercive field of over 3 T, is required so that the magnetization would remain unchanged in the opposing magnetic field. Figure 4 shows the voltage detected in synch with the modulated microwave irradiation (V_{det} , see the experimental details above and the supplementary material, available from stacks.iop.org/NJP/14/093021/mmedia) acting on SmCo_5/Cu PCs. The data are shown for two different PCs, with resistances of 24 and 29 Ω , corresponding to a contact diameter of approximately 5 nm. The microwave power is focused at the contact and is estimated to be of sufficient magnitude (photon density) to effectively induce spin-flip electron transitions in the contact core from

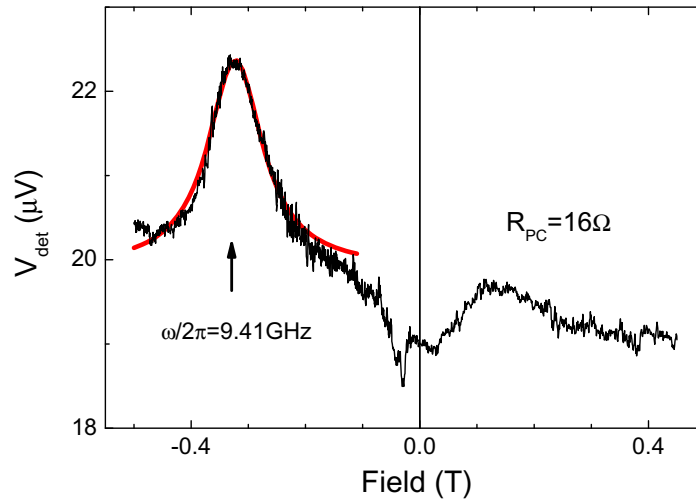


Figure 5. Detected voltage V_{det} (see text) versus magnetic field (average of two field scans) for a SmCo_5/Cu PC under microwave irradiation at 4.2 K and biased with -20 mV (electrons injected into F). The arrow indicates the resonant magnetic field H_{res} for which the photon energy $\hbar\omega = 2g\mu_s H_{\text{res}}$ for $g = 2$ and $s = 1/2$. The maximum of V_{det} at the resonance corresponds to a maximum in the PC resistance. The red (smooth) curve is a theoretical fit according to equation (1).

the low- to the high-energy Zeeman level. This overpopulates the high-energy level, thereby producing a photo-voltage (and a photo-current in the measuring circuit). The core, being a few nanometers in size, dominates the PC resistance, so even small changes in the contact core resistance can be sensitively detected. The data show a pronounced minimum when the field and the corresponding spin splitting in the normal metal match the photon energy (approximately 0.5 T for 14 GHz). These pronounced minima are absent in the absence of the microwave irradiation. The minima are unipolar in field (the signal is at the noise floor at $H = -0.5$ T), which is expected for the spin-flip process of figure 3(c) and leads to the conclusion that the minima are due to photon absorption. The minima in figure 4 are measured without a bias voltage applied to the contact, i.e. no spin injection driven by the circuit. The fact that the detector voltage is lower at the resonance, corresponding to a lower resistance at the resonance, means that the PC effectively acts as a source drawing power from the microwave field. Based on these observations, we conclude that the measured Zeeman-resonance minima are due to photon absorption by Zeeman-split spin-flip transition in the studied F/N PCs.

We next demonstrate stimulated photon emission in SmCo_5/Cu PCs in the configuration of figure 3(b), where the external field is directed along the magnetization and the bias applied injects electrons from the normal metal into the ferromagnet. The amplitude of the bias voltage is kept relatively low (-20 mV), much lower than the -70 mV range needed to excite the STT magnon instabilities (see figure 2). The data for V_{det} shown in figure 5 have a pronounced peak at approximately -0.33 T. The negative field is parallel to the magnetization, as required by the diagram of figure 3(b), and the peak is unipolar, which supports the interpretation that its origin

is the spin-flip mechanism in question. The peak is not present in the absence of the microwave irradiation, which indicates that it is stimulated in nature.

We point out that the STT excitations observed at much higher bias conditions (such as in figure 2) require neither irradiation nor external field, and in fact can be observed for both polarities of the field for the same polarity of the bias (different magnitude). The Zeeman-resonant peaks (such as in figure 5) are observed at much lower bias, do require irradiation as well as field and are unipolar in field for the low bias of the given polarity. These considerations rule out STT as an explanation of the effect observed in figure 5. Furthermore, the fact that V_{det} and therefore R_{PC} have a maximum indicates that the effective resistance of the PC core increases at resonance, which is the expected behavior for a source dissipating power through photon emission when the Zeeman resonance condition is fulfilled. Based on these experimental observations, we concluded that the effect responsible for the behavior in figure 5 is stimulated photon emission by spin-flip relaxation of inversely populated Zeeman levels in a normal metal, spin-pumped by a polarized current from a ferromagnetic injector.

In order to quantitatively model the photon resonance peaks observed, we extend our recent theory [10] to take into account spin relaxation in the PC core, which is of non-photonic origin. To do this we take the energy δ -function in the electron–photon collision integral (which determines the energy conservation law, see equation (2) in [10]) to be broadened due to spin-flip processes in the normal metal and find the relative change of the PC resistance:

$$\frac{\Delta R}{R} = \frac{4\pi\beta_{\text{tr}}^2}{3} \frac{c}{v_{\text{F}}} \frac{(\mu_{\text{B}}H_{\text{max}})^2}{\varepsilon_{\text{F}}\hbar v_{\text{sf}}} (n_0\Omega_{\text{pc}}) \left(\frac{2e^2}{h}R\right) \arctan \frac{2\xi}{1 - \xi^2 + ((\hbar\omega - 2\mu_{\text{B}}H)/\hbar v_{\text{sf}})^2}. \quad (1)$$

Here β_{tr} is the transport parameter [10], the experimental value of which is ≈ 0.3 , c and v_{F} are the light and the electron Fermi velocities, respectively, μ_{B} is the Bohr magneton, H_{max} is the magnetic component of the irradiating electromagnetic field, ε_{F} is the normal metal Fermi energy, n_0 is the electron density, Ω_{pc} is the PC volume, $\xi = \omega v_{\text{F}}/c v_{\text{sf}}$ and v_{sf} is the spin-flip rate due to spin–orbit or impurity scattering. Using v_{sf} as the fitting parameter we have fitted the above equation to the experimental data and found good agreement for $v_{\text{sf}} = 2 \times 10^9 \text{ s}^{-1}$ for the photon absorption peak of figure 4 (top curve) and $v_{\text{sf}} = 1 \times 10^{10} \text{ s}^{-1}$ for the stimulated photon emission peak of figure 5. These values correspond to a spin relaxation time of 100–500 ps, which agrees well with the typical spin relaxation time in our similarly prepared normal metal films and F/N nanodevices, measured using non-local spin injection techniques [16, 17], as well as with the data in the literature [18]. The fact that the photon peaks are broader in the case of spin pumping and emission compared to absorption can be due to the non-equilibrium situation in the spin-pumped case, where the injected hot electrons have not fully equilibrated in energy into the respective Zeeman levels before undergoing spin flip. The absorption, on the other hand, takes place from the equilibrium Zeeman-split distributions at small or zero bias.

A relatively small number of PCs, below 1% of the total number of tested contacts, showed the spectroscopic features of photon emission and absorption. This is to be compared with approximately 5–10% of PCs with STT features. The relatively low observation rate is potentially related to more stringent requirements on spin accumulation in the PC contact core in the case of photonic transition, compared to the STT case. An imperfect F/N interface can lead to a significant spin-flip scattering exciting magnons at the surface of the ferromagnet (STT) while at the same time suppressing the spin accumulation in the normal metal contact core

and thereby spin-flip photonic transition. Further progress toward spin-laser effects in metallic magnetic nanostructures should come from optimizing the microstructure and geometry of the samples and improving the efficiency of the spin-injector electrodes.

In conclusion, we have shown that a strong spin accumulation in nanometer-sized PCs between a ferromagnet and a normal metal can be accompanied by a significant spin-population inversion, which in turn may lead to stimulated spin-flip photon emission and photon absorption. The strength of the emission and absorption depends only on the total number of spin-up and spin-down electrons in the PC core, while it is independent of the distribution of electrons in momentum space (electrons' temperature). This is because photon-induced transitions between spin-up and spin-down electron states involve a negligible momentum transfer, making the kinematics of the electron–photon scattering identical to that of a two-level system formed by the spin-dependent part of the electronic energy. Two immediate consequences are that the predicted effect does not depend on the electron temperature and will not be destroyed by even strong, spin-preserving inelastic electron scattering. Our experimental observation of stimulated photon emission in ferromagnetic-normal metal PCs may in the future lead to a laser based on spin-flip electron–photon scattering in metals.

Acknowledgments

Financial support from the European Commission (FP7-ICT-FET, grant agreement no. 225955 STELE), the Swedish VR and the Korean WCU program funded by MEST/NFR (R31-2008-000-10057-0) is gratefully acknowledged. We thank V Pashchenko for measuring the low-temperature coercivity of the SmCo₅ film.

References

- [1] Baibich N, Broto J M, Fert A, Nguyen Van Dau F, Petroff F, Eitenne P, Creuzet G, Friederich A and Chazelas J 1988 *Phys. Rev. Lett.* **61** 2472
- [2] Dieny B, Speriosu V S, Parkin S S P, Gurney B A, Wilhoit D R and Mauri D 1991 *Phys. Rev. B* **43** 1297
- [3] Moodera J S, Kinder L R, Wong T M and Meservey R 1995 *Phys. Rev. Lett.* **74** 3273
- [4] Gallagher W J *et al* 1997 *J. Appl. Phys.* **81** 3741
Engel B N *et al* 2005 *IEEE Trans. Magn.* **41** 132
- [5] Zhao H B, Talbayev D, Lüpke G, Hanbicki A T, Li C H, van't Erve M J, Kioseoglou G and Jonker B T 2005 *Phys. Rev. Lett.* **95** 137202 and references therein
- [6] Viglin N A, Ustinov V V and Osipov V V 2007 *JETP Lett.* **86** 193
- [7] Kadigrobov A, Ivanov Z, Claeson T, Shekhter R I and Jonson M 2004 *Europhys. Lett.* **67** 948
- [8] Gulayev Yu V, Zilberman P E, Chigarev S G and Epshtein E M 2010 *J. Commun. Technol. Electron.* **55** 1132
- [9] Naidyuk Yu G and Yanson I K 2005 *Point-Contact Spectroscopy (Springer Series in Solid-State Sciences vol 145)* (New York: Springer)
- [10] Kadigrobov A M, Shekhter R I, Kulinich S I, Jonson M, Balkashin O P, Fisun V V, Naidyuk Yu G, Yanson I K, Andersson S and Korenivski V 2011 *New J. Phys.* **13** 023007
- [11] Singh A, Neu V, Fähler S, Nenkov K, Schultz L and Holzapfel B 2008 *Phys. Rev. B* **77** 104443
- [12] Balkashin O P, Fisun V V, Yanson I K, Triputen L Yu, Konovalenko A and Korenivski V 2009 *Phys. Rev. B* **79** 092419
- [13] Ji Y, Chen C L and Stiles M D 2003 *Phys. Rev. Lett.* **90** 106601
Chen T Y, Ji Y, Chen C L and Stiles M D 2005 *J. Appl. Phys.* **97** 10C709

- [14] Yanson I K, Naidyuk Yu G, Bashlakov D L, Fisun V V, Balkashin O P, Konovalenko A, Korenivski V and Shekhter R I 2005 *Phys. Rev. Lett.* **95** 186602
Yanson I K, Naidyuk Yu G, Fisun V V, Konovalenko A, Balkashin O P, Triputen L Yu and Korenivski V 2007 *Nano Lett.* **7** 927
- [15] Vouille C, Barthélémy A, Elokani Mpondo F, Fert A, Schroeder P A, Hsu S Y, Reilly A and Loloee R 1999 *Phys. Rev. B* **60** 6710
- [16] Poli N, Morten J P, Urech M, Brataas A, Haviland D B and Korenivski V 2008 *Phys. Rev. Lett.* **100** 136601
- [17] Urech M, Korenivski V, Poli N and Haviland D B 2006 *Nano Lett.* **6** 871
- [18] Bass J and Pratt W P Jr 2007 *J. Phys.: Condens. Matter* **19** 183201